COMMUNICATION

Supramolecular chemistry of helical foldamers at the solid-liquid interface: self-assembled monolayers and anion recognition

Received 00th January 20xx,
Accepted 00th January 20xx

DOI: 10.1039/x0xx00000x

Catherine Adam, Lara Faour, Valérie Bonnin, Tony Breton, Eric Levillain, Marc Sallé, Christelle Gautier,* David Canevet*

The synthesis of a redox-active helical foldamer and its immobilization onto a gold electrode are described. These large molecular architectures are grafted in a reproducible manner and provide foldamer-based self-assembled monolayers displaying recognition properties.

Foldamers constitute a class of synthetic oligomers that adopt well-defined and compact secondary structures.[1,2] This feature provides them with hosting abilities for a wide range of guests –be they cationic, anionic or neutral– as extensively reviewed by Ferrand and Huc,[3] Gong,[4] Jeong,[5] Li,[6,7] and collaborators. In addition, these receptors sometimes show outstanding selectivity towards specific guests,[8–11] since the shape of their inherent cavity and the electrostatic potential at the surface of the hosting pocket can be fine-tuned, through a well-selected sequence of the foldamer constituting monomers.[12]

These studies have largely been led in solution. Therefore, a major challenge that chemists are now facing consists in incorporating these molecular structures within smart materials,[13] while preserving their singular hosting properties. This definitely constitutes a demanding objective, given that intermolecular interactions may induce modifications of the three-dimensional organization, as demonstrated in the case of proteins.[14]

Herein, we propose to tackle this objective by studying self-assembled monolayers (SAMs)[15] of helical foldamers chemisorbed onto gold, since their preparation is compatible with various chemical functions, allows reaching highly organized and dense monolayers in a reproducible manner (especially with alkyl disulfide anchoring groups),[16] and was successfully used with other foldamers to produce conducting materials.[17–22]

The oligopyridine dicarboxamide foldamer backbone (Figure 1) was selected by taking into consideration 1) their well-established synthesis,[23,24] which notably allows the introduction of desired substituents on the 4-position of pyridyl rings (*e.g.* solubilizing chains or anchoring function), 2) a redox inactivity in a relatively large range of potentials,[25] 3) the moderate propensity of shorter oligomers to form dimers,[24,26,27] which constitutes a key point to favour a single helical state and 4) the presence of electropositive secondary amide protons oriented towards the center of the cavity, likely to provide the foldamer with anion recognition properties.[28,29] To follow such a supramolecular process at the solid-liquid interface, electrochemical techniques have already shown their relevance.[30–32] The binding of an anion is indeed likely to affect the local electric field and hence, to influence the redox potential of nearby electroactive probes. Thereby, the tetrathiafulvalene (TTF) unit appears well suited to probe such a binding event.[33–35] Finally, to master the complexity of the system, be that from a synthetic or an electrochemical point of view, the targeted foldamer was designed to preserve its symmetry. Therefore, TTF units were grafted at both

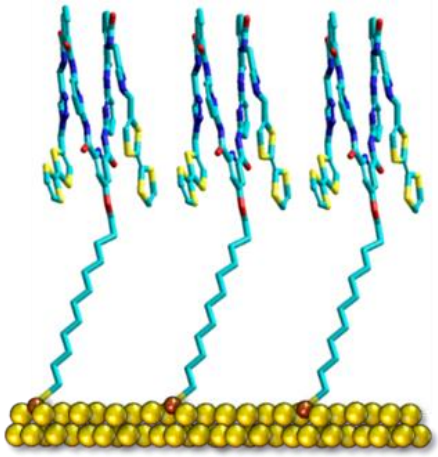

Figure 1. Schematic representation of the self-assembled monolayer based on foldamer **F**.

[a] *Laboratoire MOLTECH-Anjou, UMR CNRS 6200, UNIV Angers, SFR MATRIX, 2 Bd Lavoisier, 49045 Angers Cedex, France. christelle.gautier@univ-angers.fr, david.canevet@univ-angers.fr*

Electronic Supplementary Information (ESI) available: Experimental details, ^{1}H and ^{13}C NMR spectra, mass spectrometry information, cyclic voltammetry experiments. See DOI: 10.1039/x0xx00000x

extremities of the foldamer core and the anchoring chain was introduced on the central pyridyl ring (Figure 1).

Compound **F** displays a design, which is similar to the non-anchorable foldamer analogue described elsewhere.[36] Its synthesis (see Experimental details in the supporting information file) was performed via a multistep procedure presented in Schemes 1 and S1 and involved two major steps. The first one consisted in forming the foldamer skeleton through an acyl chloride activation of tetracarboxylic acid **S4**, which reacted with amine **S5** with an excellent yield (four amide functions generated with a 73% yield). The corresponding tetraacetylenic derivative **1** constitutes a particularly appealing precursor to graft selected building blocks through copper-catalyzed azide-alkyne cycloadditions (CuAACs) and reach foldamer-based SAMs endowed with desired properties. Herein, the CuAAC reaction was performed in the presence of azidomethyltetrathiafulvalene **2** (Scheme 1) to isolate the TTF-functionalized foldamer **F** (50% yield), whose structure was unequivocally confirmed through standard analytical techniques.

The immobilization conditions of compound **F** on gold were optimized to achieve well-defined monolayers with reproducible electrochemical behavior. Therefore, parameters such as immersion time, choice of solvent and foldamer concentration have been thoroughly optimized (see SI). Since oligopyridine dicarboxamide-based foldamers may form duplexes,[27] the chemisorption step was best performed in a dissociating solvent, dichloromethane, at low disulfide **F** concentrations in order to promote the immobilization of single helical foldamers on the surface. A foldamer **F** concentration as low as 5 µM proved sufficient to obtain a maximum surface coverage and overnight immersions were led for reaching higher degrees of organization.[15] The cyclic voltammogram of the modified surface (Figure 2) shows two redox systems centered at E_1 = 0.19 V and E_2 = 0.61 V *vs*. Ag|$AgNO_3$, which correspond to the well-described successive oxidations of neutral TTF to the $TTF^{\bullet+}$ radical cation and TTF^{2+} dication states.[35] Voltammetric analyses confirmed the confinement of the redox-active foldamers onto the gold substrate with a linear dependency of the peak intensities with the scan rate (Figure S1). The value of full width at half maximum slightly deviates from the standard 90 mV for the first redox process (145 mV), which accounts for intermolecular interactions between TTF moieties, as previously observed for TTF-based SAMs on gold surfaces.[37] These measurements also allowed determining a foldamer surface coverage of ca 3.10^{-11} mol.cm^{-2},[38] by integration of the first oxidation peak. These results suggest a close proximity between the redox units and, given the large foldamer structure, a highly compact and probably intermingled arrangement of the foldamer units at the interface.

Various helical foldamers endowed with electropositive protons inside their cavity proved to show anion recognition properties.[39] On this ground, and since the grafted foldamer includes four amide functions (see electrostatic potential map in Figure S2), the self-assembled monolayers were studied in the presence of two strongly different protic/aprotic anions (hydrogen sulfate and chloride). These analyses were led in a solution of tetrabutylammonium hexafluorophosphate (0.1 M) in dichloromethane, since this salt does not interact with the foldamer backbone.[36] As shown in Figures 3 and S3, when increasing guest concentration, the first oxidation wave was cathodically shifted by *ca.* 30 mV in the presence of chloride ions and up to 90 mV in the case of hydrogen sulfate. This assessment is especially remarkable since Fave, Schöllhorn and collaborators have recently shown that TTF-labelled self-assembled monolayers do not interact with halides upon oxidation.[40] Consequently, such a behaviour is assigned to an

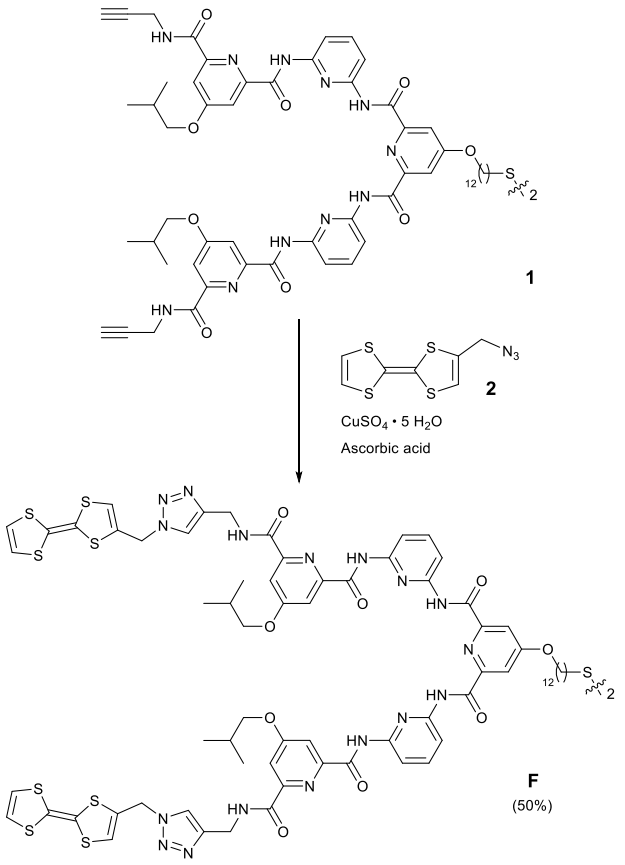

Scheme 1. CuAAC reaction leading to the synthesis of disulfide **F**.

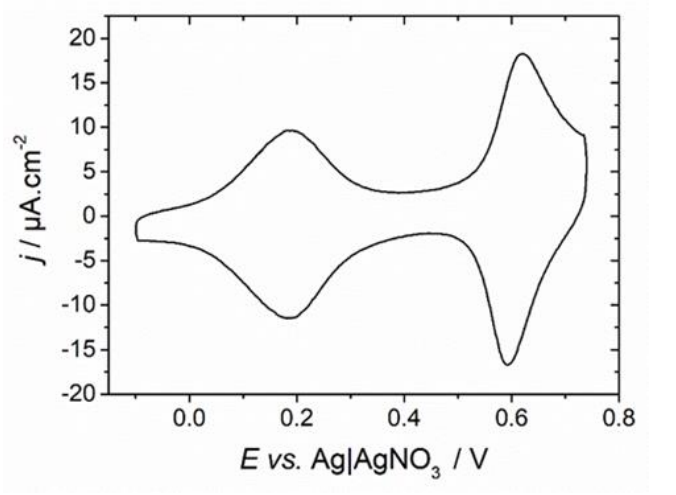

Figure 2. Cyclic voltammogram of a **F**-based self-assembled monolayer on gold electrode (nBu$_4$NPF$_6$ 0.1 M, dichloromethane, v = 100 mV.s^{-1}).

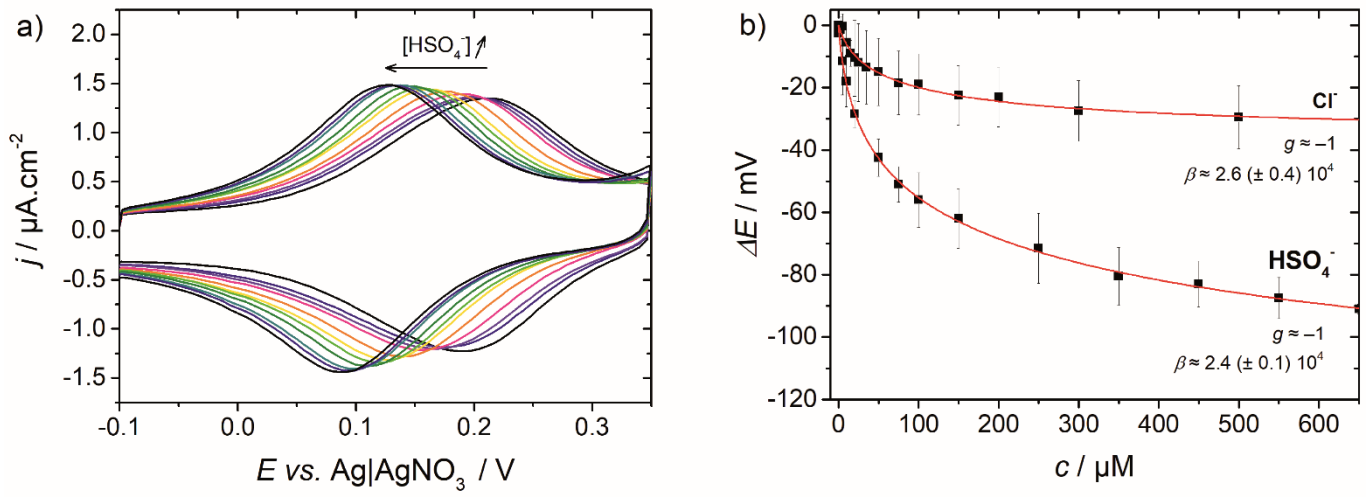

Figure 3. a) Evolution of the cyclic voltammogram of a **F**-based self-assembled monolayer (nBu$_4$NPF$_6$ 0.1 M, CH_2Cl_2) upon addition of nBu$_4$N$^+$, HSO_4^-. b) Variations of $\Delta E = E - E_i$ as a function of anion concentration (E_i stands for initial potential). Red lines correspond to the fitted Frumkin isotherms and error bars were calculated as the standard deviation on three independent measurements.

anion recognition process involving the foldamer skeleton (see Figure S5 for potential binding modes). Besides, this process explains the stabilization of the oxidized species by the negatively charged hosted ion.[34,41–43] Noteworthily, a simple flushing with dichloromethane allowed recovering the initial electrochemical response of the modified electrode, even after several cycles (Figure S4), thus confirming the reversible character of the binding process. Plotting the variation of the oxidation peak potential (ΔE) as a function of guest concentration C allowed studying the recognition phenomenon in a quantitative manner. Fitting these data through Equation (S2), which derives from the Frumkin model (see SI),[44] allows to model the observed variations of potential upon addition of anions efficiently (see Figure 3). This numerical analysis can be extended to the determination of $K_{ox}/K_{neutral}$ ratios (K_{ox} and $K_{neutral}$ stand for the binding constants in the oxidized and neutral states, respectively) according to square Scheme 2 and Equation 1. Assuming fast complexation reactions between anions in solution and immobilized foldamers, these were evaluated to $K_{ox}/K_{neutral}(Cl^-) \approx 3$ and $K_{ox}/K_{neutral}(HSO_4^-) \approx 38$, which evidences the contribution of electrostatic interactions to the binding process. When considering the recognition of charged species, ionic strength represents a parameter that may have a critical impact over the experimental observations. Consequently, we led additional experiments at respectively lower and higher supporting electrolyte concentrations (Table 1 and Figure S6). The corresponding data first evidence a strong influence of the chemical environment on the oxidation potential of TTF units, with a *ca.* 80 mV difference (from 0.153 V (C_{TBAPF_6} = 0.5 mol.L^{-1}) to 0.231 V ($C_{Bu_4NPF_6}$ = 0.01 mol.L^{-1}) *vs* Ag/AgNO$_3$). More importantly, increasing the electrolytic salt concentration (0.5 M) led to smaller ΔE variations (– 65 mV), which is consistent with stronger ion pairing, whereas a lower concentration (0.01 M) resulted in a significantly higher ΔE variation (– 135 mV). These experiments highlight to which extent the variations of oxidation potential upon anion binding depend on ionic strength. Importantly, these strong variations, as well as the extracted β constants, demonstrate that this grafted foldamer displays anion binding abilities, even at high ionic strength ($C_{Bu_4NPF_6} = 10^3 \times [HSO_4^-]$).

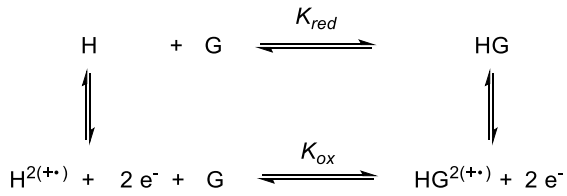

Scheme 2. Simplified square scheme gathering the binding and redox processes occurring at the interface (H stands for Host and G for Guest).

$$\ln \frac{K_{ox}}{K_{neutral}} = \frac{nF\left(E^{\circ}_{H^{2(+\bullet)}/H} - E^{\circ}_{HG^{2(+\bullet)}/HG}\right)}{RT} \qquad \textit{(Equation 1)}$$

Table 1. E_i°, ΔE and β values determined through successive additions of tetrabutylammonium hydrogen sulfate over an immersed **F**-based self-assembled monolayer (CH_2Cl_2, v = 100 mv.s^{-1}, E *vs.* Ag/AgNO$_3$) and subsequent fitting to the adapted Frumkin isotherm model.

nBu$_4$NPF$_6$ / M	E_i° (TTF) / V	E_{sat} - E_i /mV	β
0.01	0.231	– 135	6.8 (± 0.8) 10^4
0.1	0.205	– 93	2.4 (± 0.1) 10^4
0.5	0.153	– 65	1.6 (± 0.1) 10^4

In summary, a redox-active helical foldamer was specifically designed and synthesized to prepare self-assembled monolayers on gold substrate. The corresponding surface coverage and reproducible electrochemical features suggest a close packing of the foldamer molecules on the surface. To our knowledge, the recognition properties of helical foldamers once

immobilized had not been reported in the literature. Herein, we demonstrated that an oligopyridine dicarboxamide-based foldamer exhibits a hosting ability towards anions after chemisorption on gold, and that its design was relevant for the successful electrochemical transduction of a host-guest binding event. Eventually, the reversible character of the anion recognition process makes these oligomers promising candidates for the design of future stimuli-responsive materials.

Conflicts of interest

There is no conflict to declare.

Acknowledgement

The authors are thankful to the MATRIX platform for its assistance in NMR and mass spectrometry measurements. LF thanks the University of Angers for a PhD fellowship, CA acknowledges the Université Bretagne-Loire and the LUMOMAT funding program and DC is grateful to the Centre National de la Recherche Scientifique (Section 12) for a Délégation research leave.

References

1 D. J. Hill, M. J. Mio, R. B. Prince, T. S. Hughes and J. S. Moore, *Chem. Rev.*, 2001, **101**, 3893–4012.
2 S. Hecht and I. Huc, Eds., *Foldamers: Structure, Properties and Applications*, Wiley-VCH, Weinheim, 2007.
3 Y. Ferrand and I. Huc, *Acc. Chem. Res.*, 2018, **51**, 970–977.
4 K. Yamato, M. Kline and B. Gong, *Chem. Commun.*, 2012, **48**, 12142–12158.
5 H. Juwarker, J. Suk and K.-S. Jeong, *Chem. Soc. Rev.*, 2009, **38**, 3316–3325.
6 Z.-T. Li, J.-L. Hou, C. Li and H.-P. Yi, *Chem. – Asian J.*, 2006, **1**, 766–778.
7 D.-W. Zhang, X. Zhao, J.-L. Hou and Z.-T. Li, *Chem. Rev.*, 2012, **112**, 5271–5316.
8 N. Chandramouli, Y. Ferrand, G. Lautrette, B. Kauffmann, C. D. Mackereth, M. Laguerre, D. Dubreuil and I. Huc, *Nat. Chem.*, 2015, **7**, 334–341.
9 S. Saha, B. Kauffmann, Y. Ferrand and I. Huc, *Angew. Chem. Int. Ed.*, 2018, **57**, 13542–13546.
10 P. Mateus, B. Wicher, Y. Ferrand and I. Huc, *Chem. Commun.*, 2017, **53**, 9300–9303.
11 J. Kim, H. Juwarker, X. Liu, M. S. Lah and K.-S. Jeong, *Chem. Commun.*, 2010, **46**, 764–766.
12 J. Becerril, J. M. Rodriguez, I. Saraogi and A. D. Hamilton, in *Foldamers: Structure, Properties, and Applications*, Wiley-VCH, Weinheim, 2007, pp. 195–228.
13 D. J. Aitken, *New J. Chem.*, 2015, **39**, 3188–3189.
14 P. Roach, D. Farrar and C. C. Perry, *J. Am. Chem. Soc.*, 2005, **127**, 8168–8173.
15 J. C. Love, L. A. Estroff, J. K. Kriebel, R. G. Nuzzo and G. M. Whitesides, *Chem. Rev.*, 2005, **105**, 1103–1170.
16 P.-Y. Blanchard, G. T. Kenfack, E. Levillain and C. Gautier, *ChemistrySelect*, 2016, **1**, 3171–3174.
17 S. K. Dey, Y.-T. Long, S. Chowdhury, T. C. Sutherland, H. S. Mandal and H.-B. Kraatz, *Langmuir*, 2007, **23**, 6475–6477.
18 K. Yamamoto, H. Sugiura, R. Amemiya, H. Aikawa, Z. An, M. Yamaguchi, M. Mizukami and K. Kurihara, *Tetrahedron*, 2011, **67**, 5972–5978.
19 M. Carini, M. P. Ruiz, I. Usabiaga, J. A. Fernández, E. J. Cocinero, M. Melle-Franco, I. Diez-Perez and A. Mateo-Alonso, *Nat. Commun.*, 2017, **8**, 15195.
20 A. Méndez-Ardoy, N. Markandeya, X. Li, Y.-T. Tsai, G. Pecastaings, T. Buffeteau, V. Maurizot, L. Muccioli, F. Castet, I. Huc and D. M. Bassani, *Chem. Sci.*, 2017, **8**, 7251–7257.
21 K. Pulka-Ziach and S. Sęk, *Nanoscale*, 2017, **9**, 14913–14920.
22 K. Pulka-Ziach, A. K. Puszko, J. Juhaniewicz-Debinska and S. Sek, *J. Phys. Chem. C*, 2019, **123**, 1136–1141.
23 I. Huc, *Eur. J. Org. Chem.*, 2004, 17–29.
24 B. Baptiste, J. Zhu, D. Haldar, B. Kauffmann, J.-M. Léger and I. Huc, *Chem. – Asian J.*, 2010, **5**, 1364–1375.
25 F. Aparicio, L. Faour, M. Allain, D. Canevet and M. Sallé, *Chem. Commun.*, 2017, **53**, 12028–12031.
26 H. Jiang, V. Maurizot and I. Huc, *Tetrahedron*, 2004, **60**, 10029–10038.
27 V. Berl, I. Huc, R. G. Khoury, M. J. Krische and J.-M. Lehn, *Nature*, 2000, **407**, 720–723.
28 P. D. Beer and P. A. Gale, *Angew. Chem. Int. Ed.*, 2001, **40**, 486–516.
29 N. Busschaert, C. Caltagirone, W. Van Rossom and P. A. Gale, *Chem. Rev.*, 2015, **115**, 8038–8155.
30 N. H. Evans and P. D. Beer, *Angew. Chem. Int. Ed.*, 2014, **53**, 11716–11754.
31 S. Zhang, C. M. Cardona and L. Echegoyen, *Chem. Commun.*, 2006, 4461–4473.
32 N. H. Evans, H. Rahman, J. J. Davis and P. D. Beer, *Anal. Bioanal. Chem.*, 2012, **402**, 1739–1748.
33 K. A. Nielsen, W. S. Cho, J. O. Jeppesen, V. M. Lynch, J. Becher and J. L. Sessler, *J. Am. Chem. Soc.*, 2004, **126**, 16296–16297.
34 B.-T. Zhao, M.-J. Blesa, N. Mercier, F. Le Derf and M. Sallé, *New J. Chem.*, 2005, **29**, 1164–1167.
35 D. Canevet, M. Sallé, G. Zhang, D. Zhang and D. Zhu, *Chem. Commun.*, 2009, 2245–2269.
36 L. Faour, C. Adam, C. Gautier, S. Goeb, M. Allain, E. Levillain, D. Canevet and M. Sallé, *Chem. Commun.*, 2019, **55**, 5743–5746.
37 P.-Y. Blanchard, O. Alévêque, S. Boisard, C. Gautier, A. El-Ghayoury, F. Le Derf, T. Breton and E. Levillain, *Phys. Chem. Chem. Phys.*, 2011, **13**, 2118–2120.
38 O. Alévêque, P.-Y. Blanchard, T. Breton, M. Dias, C. Gautier and E. Levillain, *Electrochem. Commun.*, 2012, **16**, 6–9.
39 H. Juwarker and K.-S. Jeong, *Chem. Soc. Rev.*, 2010, **39**, 3664–3674.
40 H. Hijazi, A. Vacher, S. Groni, D. Lorcy, E. Levillain, C. Fave and B. Schöllhorn, *Chem. Commun.*, 2019, **55**, 1983–1986.
41 K. Heuzé, C. Mézière, M. Fourmigué, P. Batail, C. Coulon, E. Canadell, P. Auban-Senzier and D. Jérome, *Chem. Mater.*, 2000, **12**, 1898–1904.
42 B. T. Zhao, M. J. Blesa, F. Le Derf, D. Canevet, C. Benhaoua, M. Mazari, M. Allain and M. Sallé, *Tetrahedron*, 2007, **63**, 10768–10777.
43 H. Lu, W. Xu, D. Zhang, C. Chen and D. Zhu, *Org. Lett.*, 2005, **7**, 4629–4632.
44 J. G. Vos, R. J. Forster and T. E. Keyes, *Interfacial Supramolecular Assemblies*, Wiley, Chichester, 2003.

